https://doi.org/10.33472/AFJBS.6.Si3.2024.399-412

African Journal of Biological Sciences

Journal homepage: http://www.afjbs.com

Research Paper Open Access

FELBAMATE CHITOSAN NASAL NANOSUSPENSION: AN *IN-VITRO* AND *IN-VIVO* EVALUATION

Poonam Maurya[1,2], Rishikesh Gupta[1*], Alok Mahor[1]

[1]Institute of Pharmacy, Bundelkhand University, Jhansi, U.P., India 284128

[2]Shambhunath Institute of Pharmacy, Prayagraj, U.P., India 211015

*Corresponding Author: rishikeshgupt@gmail.com

Volume 6, Issue Si3, 2024

Received: 7 April 2024

Accepted: 05 May 2024

doi: 10.33472/AFJBS.6.1.2024.399-412

ABSTRACT

Since the early nineties, felbamate has been utilized as an effective treatment for refractory partial seizures (with or without generalization). Felbamate's risk of idiosyncratic aplastic anaemia and hepatotoxicity has limited its use. Its highly reactive metabolites are the cause of hepatotoxicity and aplastic anaemia. The study formulated a nose-to-brain felbamate chitosan nanosuspension to increase brain uptake and avoid first-pass metabolism so as to remove risk factors associated with felbamate oral therapy. Felbamate nanosuspension was prepared using chitosan as a mucoadhesive polymer by ionic gelation with magnetic stirring and sonication. Using a micropipette (10-100 µL), the produced nanosuspension was injected into the rats' nostrils, allowing the drug to travel directly from the nose to the brain. The optimized formulations exhibited a bluish transparent appearance, a mean particle size of 115.0 ± 4.37 nm, a PDI of 0.118 ± 0.02, a zeta potential of +34.0 6 ±1.3 mV, and an entrapment efficiency of 90.32%. Felbamate concentration in brain homogenate was calculated using UV/VIS Spectrophotometer. When given as a suspension, felbamate concen6trations in the brain and plasma were 112.56 ± 17.81 and 401.62±20.92 ng/ml, respectively; however, when given as a nanosuspension, these values increased to 400.34±23.67 and 451±21.12 ng/ml, respectively ($p < 0.05$) after intranasal administration of the same dose. Animals given nanosuspension at several doses showed less amount of drug in other body organ compared to brain and thus targeting of drug to brain and reduce side effects associated with it. These findings suggest that the felbamate-chitosan nanosuspension was stable, safe, and capable of delivering drug to the brain via nasal route without any harm to other organs and in controlled manner and may be considered as a promising alternative route for oral drug delivery for management of refractory seizures.

Keywords: Felbamate; chitosan; mucoadhesive nanosuspension; antiepileptic; nose to brain targeting

1. Introduction:

In epilepsy, abnormal brain activity causes seizures and, in extreme cases, coma. Seizures that occur often and without warning are hallmarks of epilepsy, which is caused by an imbalance between excitatory and inhibitory actions in the central nervous system. Fifty million people worldwide have epilepsy, with eighty percent residing in underdeveloped countries. About 30% to 40% of people with epilepsy will not respond to treatment. The physical, mental, social, and financial costs of refractory epilepsy are high (Thakkar et al. 2015).

Felbamate, a broad-spectrum antiepileptic drug, is effective in treating refractory partial seizures, with or without generalization. In the 1980s, the anti-epileptic effects of felbamate were discovered. In 1993, the US Food and Drug Administration approved its use for treating adults experiencing partial-onset seizures and Lennox-Gastaut syndrome (Cilio, Kartashov, and Vigevano 2001; Schmidt 1993; Siegel et al. 1999). Instances of aplastic anaemia led to its removal from the market in August 1994. The "Black Box" warning about felbamate's link to aplastic anaemia and hepatic failure severely limited its application (Cilio, Kartashov, and Vigevano 2001; French et al. 1999). The first generic version of felbamate was given US approval in 2011. Felbamate is marketed as tablets (400 mg and 600 mg) and as a peach-coloured oral suspension (600 mg/5 mL). Research and clinical use of felbamate throughout the years have uncovered a number of safety issues (Borowicz et al. 2004). 33% of patients with aplastic anaemia had an autoimmune disease, 42% of felbamate patients had a history of cytopenia, and 52% of patients had a history of allergy or severe toxicity to another AED, according to research (Thakkar et al. 2015). Therefore, these diseases should be evaluated before starting felbamate treatment. One in 7,000 to 1 in 22,000 people who take felbamate will experience fatal hepatotoxicity. This is equivalent to other anti-convulsant drugs like valproate(Thakkar et al. 2015).

Intra nasal administration of felbamate can be used in both chronic and emergency treatments and be potentially performed either inside or outside the hospital environment. It also bypasses the hepatic metabolism and directly transfer the drug to brain (Agrawal et al. 2018) thus intranasal drug delivery of FBM may bypasses the liver damage and other safety concerns related to this drug. The goal of this research was to improve the efficacy of felbamate medication for the management of epilepsy by resolving concerns related to its oral delivery and other systemic adverse effects.

2. MATERIAL AND METHODS

2.1 MATERIALS

Felbamate (Fb) was obtained as a gift sample from Merck Ltd., Mumbai, India. Chitosan was purchased from Wanbury Ltd. Mumbai, India. Tripolyphosphate obtained from Aldrich Chemicals, UK. From S D Fine Chemicals Ltd, Mumbai, India, acetic acid and sucrose were bought. From Baroda Chemical Industries Ltd., Vadodara, India, ethanol was purchased. All additional chemicals and solvents were of analytical quality and were utilized without further purification.

2.2 ANIMALS:

Male adult Albino Wistar rats weighed between 200 and 250 g were used in the present *in-vivo* study. Institutional Animal Ethical Committee (IAEC), Bundelkhand University (Approval No. is BU/Pharma/IAEC/A/22/04) approved the protocol for in vivo experiments. Under the permitted criteria (temperature 22±3°C; relative humidity of 30%-70%), the animals were

housed in polypropylene cages with six individuals. Each animal was provided with a regular diet of laboratory food and access to water at all times.

2.3 FORMULATION OF FBM LOADED CHITOSAN NANOSUSPENSION:

Ionic gelation method was utilized to formulate felbamate-loaded chitosan nanoparticles (FNPs), with a few minor changes from the procedure published by Bhattamisra et al. (2020). In this method, we first prepared 10 ml of a homogeneous solution of chitosan in aqueous acetic acid (1.5 % v/v). Then slowly added Felbamate solution (in PEG 400) and tween 80 to the chitosan solution while stirring constantly for about 30 minutes at 300 rpm. To produce Felbamate nanoparticles, dropwise mix the cross-linker sodium tripolyphosphate solution in distilled water into the chitosan solution containing Felbamate for 20 minutes at room temperature using a magnetic stirrer at 1000 rpm. Different formulations were prepared by changing polymer concentration, polymer to crosslinker ratio and surfactant concentration. The entrapment efficiency was calculated by collecting the supernatant after ultracentrifuging the resulting FNPs at 15,000 rpm for 30 minutes at 4 °C. A cryoprotectant (D-Mannitol 2%, w/v) was applied prior to freeze-drying in order to create freeze-dried NPs. These NPs were then stored for further characterization studies.

2.4 CHARACTERIZATION OF FNPs:

2.4.1 % Drug loading

The dried FNPs (5 mg) were put into a volumetric flask measuring 25 ml. The FNPs were dissolved by adding 10 ml of distilled water and sonicating the mixture for 15 minutes. After the nanosuspension was made, it was filtered using a millipore syringe filter. The amount of Felbamate in distilled water was determined by UV/VIS Double beam spectrophotometer (Alam et al. 2012; Bhavna et al. 2014). The percent drug loading (% DL) calculated by the following equation:

$$\%\ DL\ = \frac{Amount\ of\ the\ drug\ in\ particles}{total\ amount\ of\ nanoparticles} X100 \qquad (1)$$

2.4.2 Entrapment Efficiency

The technique described by Bhattamisra et al. (2020) was used to measure nanoparticle-encapsulated Felbamate. Measuring the amount of free Felbamate in the aqueous supernatant medium allowed for an indirect evaluation of the entrapped Felbamate in FNPs. In this test, 10 mL of FNPs were concentrated by ultracentrifugation at 20,000 rpm for 60 minutes at 4°C. To determine the presence of the free drug in the solution, the ultracentrifuged supernatant was diluted and UV spectrophotometrically analyzed (at wavelength 210 nm). Utilizing the Felbamate standard curve, the precise free drug concentrations were determined. The percentage of EE was calculated using the formula below:

$$EE = \frac{Initial\ weight\ of\ drug\ (mg) - Free\ drug\ in\ supernatant\ (mg)}{Initial\ weight\ of\ drug\ (mg)} X100 \qquad (2)$$

2.4.3 Shape and Surface morphology of FNPs:

The structure and surface morphology of FNPs were studied using scanning electron microscopy (SEM). The sample was created by sparingly scattering the NPs on a double adhesive carbon tape, which was subsequently affixed to a metallic stub and coated. Scanning

electron microscopy (Leo435 VP, Cambridge, UK) at 15 keV was used to examine the stub after it had been coated with gold to a thickness of about 10 nm using a sputter coater in an argon-atmosphere high-vacuum evaporator.

Transmission electron microscopy (TEM) was used to investigate the morphology and structure of the optimized FNPs. A drop of FNPs was deposited on a copper grid, and after 20 seconds, the grid was stained with phosphotungstate for TEM examination. The surplus solution was drained off and was left to air dry for 10 minutes at room temperature. After the sample was dry, it was focused onto a sheet of photographic film. Digital micrographs and a soft imaging viewer were used to acquire and analyze the images (Kaur et al. 2018).

100µl aliquots from all nanosuspension batches were diluted with distilled water (900µl) and average particle size and polydispersity index were measured by Zeta sizer (Malvern Instruments, UK) at 25°C under a fixed scattering angle of 90°. All experiments were performed thrice (n=3). The zeta potential was measured by taking an average of 30 observations in triplicate.

2.4.4 X-ray diffractometric analysis

An X-ray diffractometer (PAN analytical, X'Pert Pro model, Germany) was used to take measurements of the powder diffraction patterns of Fb, chitosan, and optimized FNPs. The samples were scanned from 5° to 90° (2θ) using Cu Ka radiation (45 kV, 40 mA). The automatic divergence slit assembly and proportional detector were used, and the scanning speed was 2°/min. All samples were scanned at the temperature of 25° C (Seju, Kumar, and Sawant 2011).

2.4.5 Fourier Transform Infrared (FTIR) Spectra of FNPs:

FT-IR spectrophotometer (Shimadzu Corporation, Japan) was used to record the FTIR spectra of chitosan and FNPs on KBr pellets.

2.4.6 In vitro drug release study

The dialysis technique was used to assess the in vitro release of Fb from FNPs at a temperature of 37±0.5°C with a 100 rpm agitation rate. A suspension of FNPs (2 ml) was put into a dialysis bag, sealed at both ends, and put into dissolution vessels with 150 ml of PBS of pH 7.4. At predetermined intervals (0.5, 1, 2, 4, 6, 8, 12 and 24 h), remove the samples (1 ml) and replace them with the same volume of fresh release medium to keep the volume constant. The samples were filtered with Millipore before being tested for felbamate at 210 nm with a UV/VIS Double Beam spectrophotometer. The same procedure was followed for FBM suspension (Liu, Yang, and Ho 2018).

2.4.7 Nasal ciliotoxicity study

Franz diffusion cells were mounted to three identically sized pieces of nasal mucosa (0.2 mm). As a positive control, the first portion of mucosa (A) was exposed for 1 hour to isopropyl alcohol (a mucociliary toxic agent). The second (B) and third (C) mucosal samples were treated for 1 hour with PBS (pH 6.4) and FNPs, respectively. Following a one-hour wash in PBS (pH 6.4), all three mucosa samples were immersed overnight in a 10% v/v formalin solution. Each mucosa was sliced to a depth of 5 mm using a microtome. To assess any harm to the nasal mucosa, slides were prepared, stained with hematoxylin and eosin, and inspected under an inverted microscope (Olympus- IX51, USA) (Wen et al. 2011).

2.4.8 Estimation of drug content in the brain and plasma

For this research, albino wistar male rats weighing between 200±10 g were chosen. The animals were separated into two groups (A and B), each with n=6. Wistar rats in Group A and Group B were administered Fb suspension (7.14 mg) and Fb nanoparticle formulation (FNPs) (equivalent to 7.14 mg of Fb) respectively through each nostril using a micropipette. Prior to nasal administration, animals were restrained in a slanted position and anesthetized with pentobarbital sodium (35-50 mg/kg i.p.). At various time intervals (1, 2, 4, 8, and 24 h), rats were sacrificed by pentobarbital sodium overdose, and blood was extracted via heart puncture. The blood was collected and centrifuged, and the supernatant was stored at -21 ℃ for further UV/VIS spectrophotometric analysis. After that brains were separated and rinsed twice with normal saline, adherent tissue/fluid was removed, and the brain was weighed. After weighing, it was homogenized in a 1:5 ratio of brain weight to normal saline solution. For further drug investigation using a UV/VIS Spectrophotometer, the supernatant was collected after centrifuging the homogenate at 4000 rpm for 20 minutes at 4 °C. The drug concentrations in the plasma and brain were calculated using the liquid-liquid UV/VIS Spectrophotometric technique, which was carried out to the clear supernatant. Pharmacokinetic software (PK Functions for Microsoft Excel, Pharsight Corporation, Mountain View, CA, USA) was used to investigate the pharmacokinetic parameters of Fb after i.n. (Fb sus.) and i.n. (FNPs) administration. Graph pad prism 9.0 (Graph pad software, San Diego, CA) was used for the calculation and statistical analysis of the pharmacokinetic parameters C_{max}, T_{max}, $AUC_{0-\infty}$, $AUMC_{0-\infty}$, mean residence time (MRT) and elimination rate constant (Ke). Analysis of variance (ANOVA) was used, and then the Tukey-Kramer multiple comparison analysis was used to evaluate the significance of the observed group differences. Statistical significance was defined as a P-value less than 0.05, and all data are shown as the mean ± standard deviation. (Fazil et al. 2012; Haque et al. 2012; Xiao et al. 2016).

2.4.9 Biodistribution Studies

The amount of drug that reaches the intestines, liver, kidney, lungs, brain, and blood was studied through biodistribution experiments. To examine biodistribution, adult male Albino Wistar rats (weighing 200-250 g) were used. Before being randomly split into two groups of six rats each, all of the rats were ear-tagged with a picric acid solution. Each formulation at each time point was tested three times. The FNPS formulation or the control Fb suspension containing 7.14 mg Fb (equal to 35.70 mg/kg body weight) was delivered in each nostril using a micropipette (10-100 L). During nasal delivery, the rats were held upright from behind. At 1, 2, 4, 8, and 24 hours post-sacrifice, the cardiac puncture was used to draw blood from each rat. Following the withdrawal of blood, the brain and other organs (such as the liver, intestine, lungs and kidney) were separated and rinsed twice with normal saline to remove any adhering tissue or fluid, then placed in vials and weighed. UV/VIS Double beam spectrophotometer was used to determine the amount of Fb in each organ or tissue. The amount of Fb that accumulated per milligram in each organ or tissue was reported as a percentage of the dosage given per milligram of tissue (% AD/ mg Organ). Two-way ANOVA was used for statistical analysis to compare the data (Tong, Qin, and Sun 2017; Wen et al. 2011).

2.4.10 Statistical Analysis

Results with a p-value of less than 0.05 from the Student's t-test were regarded to be statistically significant. Unless otherwise specified, all reported data are presented as means ± standard deviations.

3. RESULT AND DISCUSSION

3.1 FORMULATION AND CHARACTERIZATION OF FNPs

The ionic gelation process was slightly modified to create the Felbamate-loaded chitosan nanoparticles (FNPs) (Tzeyung et al. 2019). The synthesis of chitosan nanoparticles is based on the ionic gelation interaction between (+)ve charged chitosan and (-)ve charged tripolyphosphate (TPP) at ambient temperature. TPP is a multivalent anion with negative charges, and the amino groups in chitosan in an acidic solution make it vulnerable to protonation. Using electrostatic repulsion and attraction, TPP was able to bind to the $NH3^{+}$ groups in chitosan, resulting in ionically crosslinked chitosan nanoparticles. Data on the generated NPs' mean particle size, particle distribution index, zeta potential, shape, and drug entrapment efficiency were analyzed.

The zeta sizer analysis showed that the average particle size of the produced optimized NPs was 115.0 ± 4.37 nm. Particle size distribution is also uniform, as seen by the PDI value (0.118 ± 0.02) being less than 0.5. As shown in Figure 1, the zeta potential for the NPs was measured to be +34.0 mV, indicating good stability. The positive zeta potential of chitosan is caused by a leftover amino group on its molecules that is not neutralized after the crosslinking of TPP molecules.

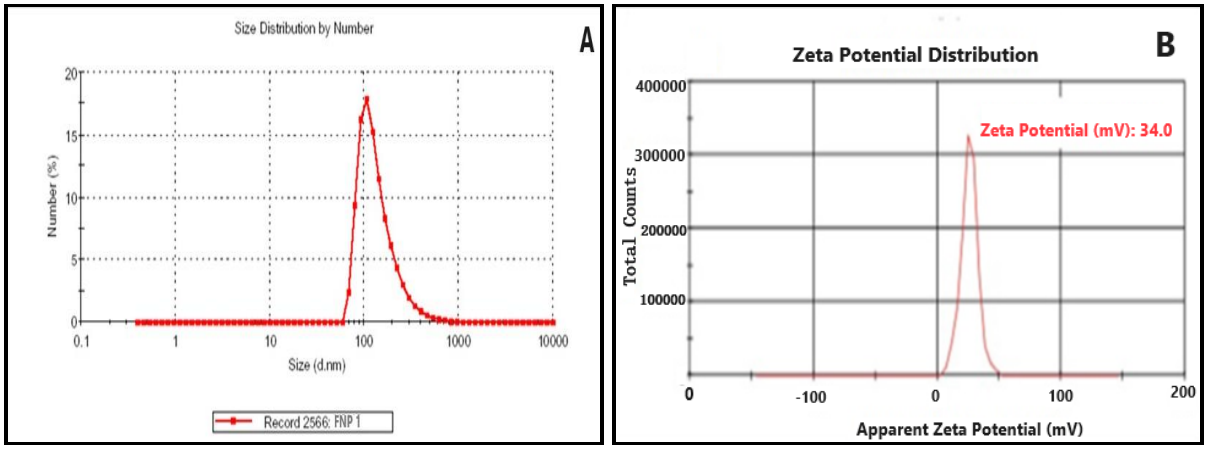

Figure 1. (A) Average particle size distribution, (B) Average Zeta potential of prepared FNPs.

The FNPs were analyzed by TEM and FESEM, both of which showed that their sizes were less than 100 nm and that their surfaces were smooth and uniform (Figures 2 and 3). If we want NPs to make it from our nose to our brain, they need be less than 200 nm. In terms of cellular absorption, drug release, and biodistribution, particle size is crucial.

Therefore, the formulation's appropriateness for intranasal delivery was confirmed by the produced NPs' having particle size < 200 nm, small PDI, satisfactory zeta potential, and entrapment efficiency.

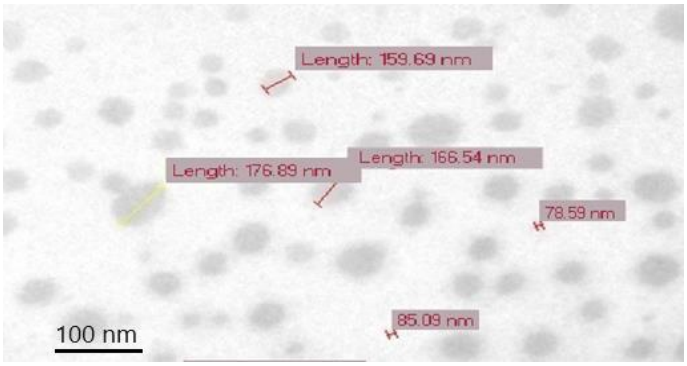

Figure 2. *TEM photomicrograph of prepared FNPs*

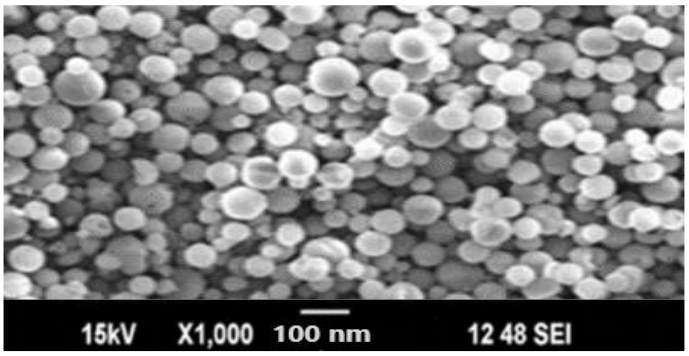

Figure 3. *FESEM photomicrograph of prepared FNPs*

3.2 X-RAY DIFFRACTOMETRIC ANALYSIS

Figure 3 displays an X-ray diffraction (XRD) comparison between Felbamate, chitosan, physical mixture, placebo chitosan NPs, and FNPs. Peaks at 2θ of 9º and 20.43º (Figure 4) are characteristic of chitosan, demonstrating its high degree of crystallinity. Pure Felbamate has a prominent peak at 2θ at 10.29º and 19º, which is a defining feature of the compound. No drug-polymer interaction was observed in the physical mixture of chitosan and Felbamate, as evidenced by the presence of peaks. Crystallinity decreases when peak intensities and peak widths differ from those of the individual diffraction pattern. The weakly crystalline structure of the placebo chitosan NPs was evidenced by a single diminished peak of CS at 9º in the diffraction pattern. The crystallinity of Felbamate was decreased as seen by the expansion of the peaks at 10.29º and 19º in FNPs. The diffraction pattern of FNPs showed significantly reduced or absent intensities for felbamate due to the cross-linking among CS and TPP, where Felbamate was entrapped.

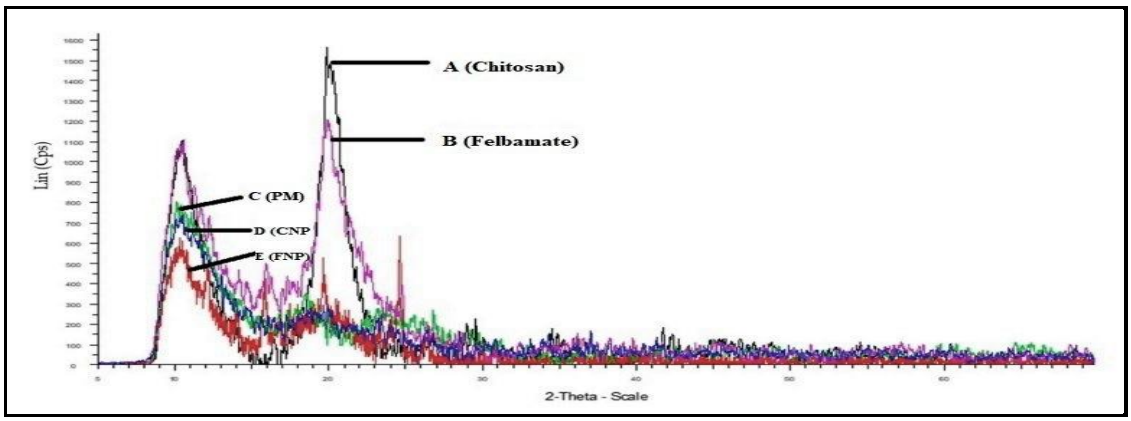

Figure 4. X-ray diffraction pattern of (A) chitosan, (B) Felbamate, (C) physical mixture of chitosan and Felbamate, (D) Chitosan NPs, and (E) FNPs.

3.3 FOURIER TRANSFORM INFRARED (FTIR) SPECTRA STUDIES

FTIR spectra of chitosan and FBM-encapsulated chitosan nanoparticles are shown in Figure 5. The amide I band, N-H bending, and C-N stretching are the three most prominent absorption bands in chitosan, with their respective center frequencies of (1700-1600) cm−1, (1500-1550) cm−1, and (2800-2900) cm−1. Figure 2 shows that due to the significant ionic crosslinking of chitosan and TPP, the amide I band and the N-H bending have been greatly displaced to 1570 (N-H stretching vibration of NH3+ group) and 1406 cm−1, respectively. The appearance of peaks at 1364 cm−1 (aromatic ring), 771 cm−1 (vibration of CF=CH group), and 3000-3500 cm−1 (more F (unbound) groups from the Felbamate) strongly indicated efficient encapsulation of Felbamate into chitosan nanoparticle.

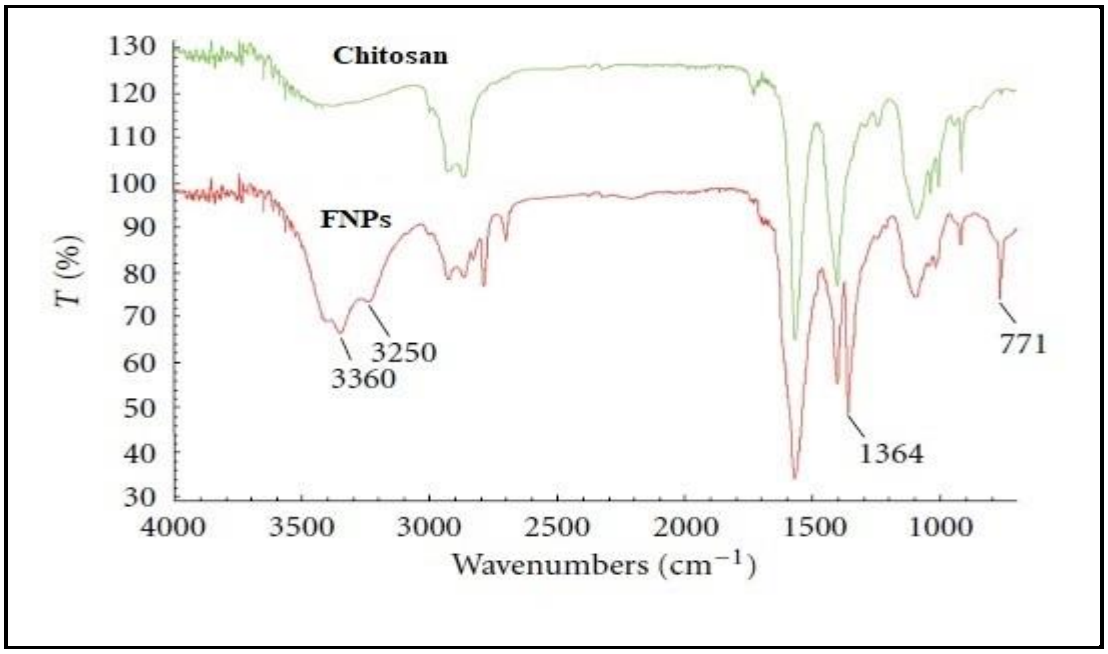

Figure 5. FTIR spectra of Chitosan and Felbamate encapsulated chitosan nanoparticles

3.4 IN VITRO RELEASE OF FELBAMATE FROM FNPs

Using a release medium (phosphate buffer 7.4), chitosan nanoparticles were incubated and their Felbamate release behaviour was evaluated using UV spectrophotometry. The release profiles of felbamate are shown in Figure 6 for incubation times of up to 48 hours. After 2 hours, 12.23 ± 2.87 percent of the drug had been released in the case of pure Fb suspension. In Figure 6, we can see that the initial burst release of Felbamate from chitosan nanoparticles was 49.01 1.31% after 2 hours in all incubation media. Felbamate was initially rapidly released, defined as a "burst effect," because some amounts were concentrated on the surface of nanoparticles via adsorption and were then easily released via diffusion. The total amount released over the incubation period is 99.38 ± 4.24%, after an initial burst effect that was followed by a slower sustained, and controlled release. Felbamate molecules were absorbed onto the exterior surfaces of the chitosan nanoparticles, and their release patterns confirmed that they were contained among the positively charged hydrophilic chains.

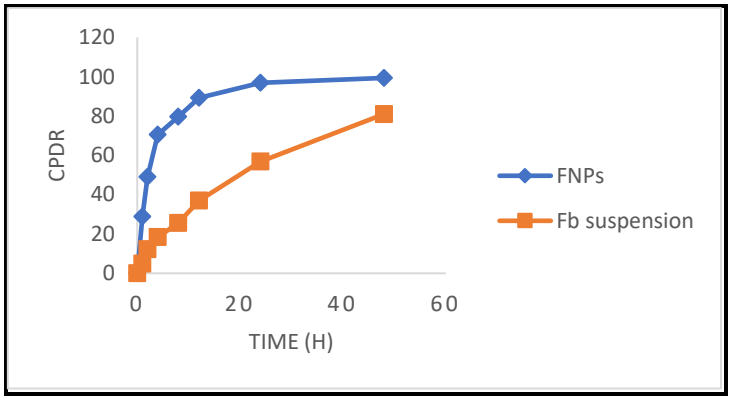

Figure 6. Cumulative percentage drug release from Fb suspension and FNPs.

3.5 NASAL CILIOTOXICITY STUDY

The formulation excipients were tested for nasal ciliotoxicity to determine if they posed any threat to the nasal mucosa. As can be seen in Figure 7 (A), the epithelial layer of the goat nasal mucosa was destroyed and interior nasal tissues were damaged after being exposed to the positive control, isopropyl alcohol. Intact epithelial layer and no nasociliary damage in nasal mucosa treated with negative control PBS pH 6.4 (Figure 7 B) and with FNPs (Figure 7 C) showed the safety of excipients employed in the chitosan.

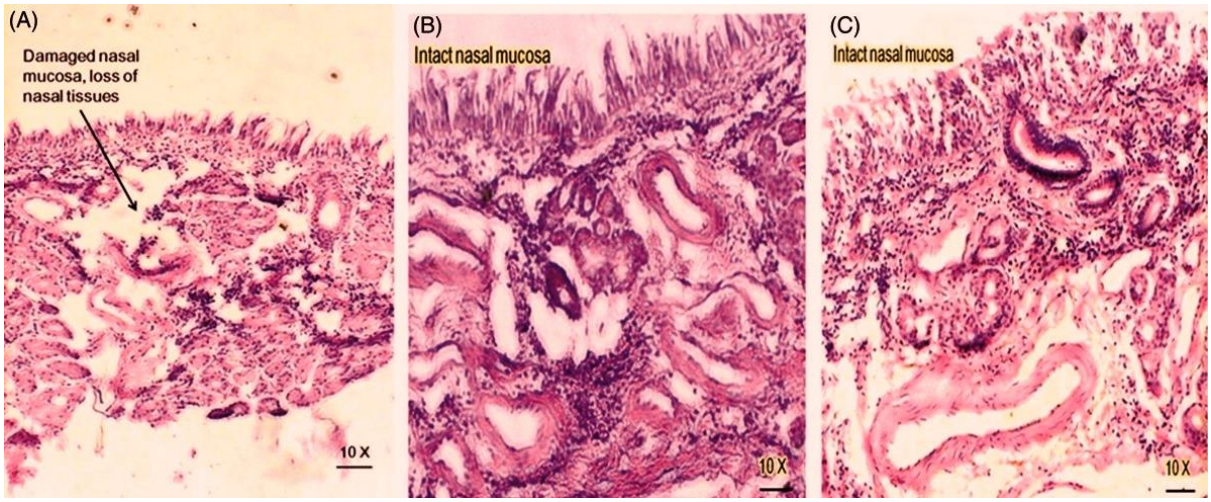

Figure 7. Optical microscopic images of nasal mucosa. (A) Positive control – isopropyl alcohol, (B) Negative control – PBS (pH 6.4) and (C) FNPs treated mucosa.

3.6 ESTIMATION OF DRUG CONTENT IN THE BRAIN AND PLASMA

When comparing brain Fb concentrations before and after i.n. administration of FNPs and Fb suspension, a statistically significant (P 0.05) rise was seen after i.n. administration of FNPs. Figure 8 shows the concentration of Fb in the blood and brain over time after intranasal administration of FNPs (a) and Fb suspension (b). The several Fb pharmacokinetic parameters were calculated using Pharmacokinetic Functions for Microsoft Excel, and the results are shown in Table 1. The shorter T_{max} for the brain (2 h) compared to blood (4 h) after intranasal treatment suggests a preference for transport via the nose to the brain. When compared to C_{max} in the brain after intranasal administration of Fb suspension (400.34 23.67 ng/mL), C_{max} in the brain after intranasal administration of FNPs was significantly (P 0.05) greater. FNPs i.n. had a substantially ($P < 0.05$) greater $AUC_{0-\infty}$ than Fb suspension (i.n.), with a value of 3381.64 ± 66.72 ng.h/mL. Possible explanations include the BBB's avoidance and direct drug transfer

via the olfactory pathway. FNPs i.n. had an $AUC_{0-\infty}$ in the brain that was about 2.42 times that of Fb suspension. i.n.

The percent relative bioavailability of intranasally supplied FNPs in blood and brain was 234.13±13.45 and 402.92±21.92, respectively, compared to i.n. administered Fb-suspension (Table 1). After being given FNPs via the nasal route, the bioavailability of Fb in the brain was shown to increase significantly ($P < 0.05$).

Table 1. Brain and Plasma Fb Pharmacokinetic Parameters Following Intranasal administration of FNPs and Fb Suspension Instilled into Rats' nostril

Parameter	**FNPs i.n.**		**Fb suspension i.n.**	
	Brain	**Plasma**	**Brain**	**Plasma**
C_{max}* *(ng/mL)	400.34±23.67	451±21.12	112.56±17.81	401.62±20.92
T_{max}* *(h)	2	5	2	1
AUC_{0-24h} (ng·h/mL)	3128.81±55.56	3382.34±61.82	1229.72±50.73	2012.63±49.18
$AUC_{0-\infty}$ (ng·h/mL)	3381.64±66.72	3429.82±69.31	1392.77+58.84	2211.73±61.12
$AUMC_{0-24h}$ ($ng \cdot h^2/mL$)	14561.73±60.63	16711.46±66.73	6871.34±56.81	10837.81±62.84
$AUMC_{0-\infty}$ (ng·h/mL)	16729.63±62.82	18928.73±68.92	7018.73±60.23	12001.76±67.29
K_e* *(h^{-1})	0.082±0.0073	0.098±0.0069	0.074±0.0062	0.123±0.0071
MRT (h)	14.72±1.01	7.82±0.91	10.34±0.89	9.92±0.91
RB (%)[a]	402.92±21.92	234.13±13.45		

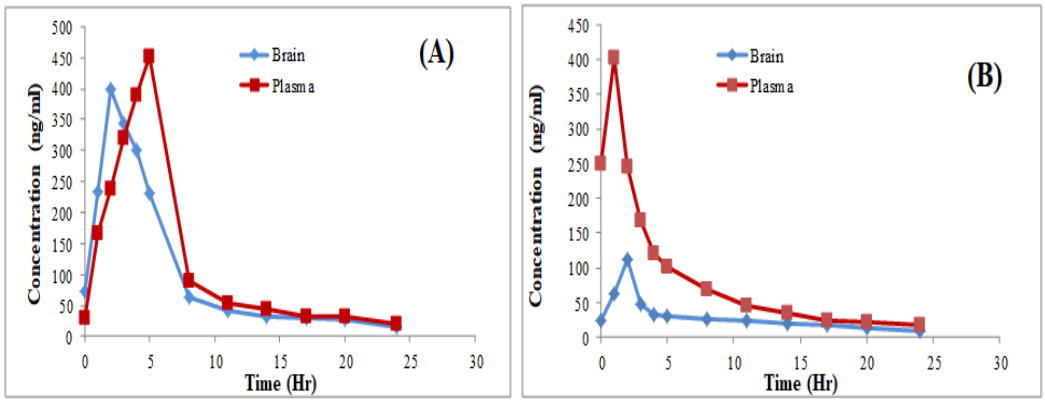

Figure 8. Drug Conc. versus Time Profile of Fb in Brain and in Plasma after administration of (A) FNPs i.n.; (B) Fb suspension i.n.

3.7 BIODISTRIBUTION STUDIES

The biodistribution of FNPs and Fb suspension following intranasal delivery was studied in a variety of tissues at 1, 2, 4, 8, and 24 hours (Figure 9 and 10). Figure 10 depicts the distribution of Fb after intranasal administration of the positive control (Fb suspension), and Figure 9 depicts the distribution of Fb following intranasal administration of FNPs.

Brain Fb levels were consistently and significantly ($P < 0.01$) higher after i.n. administration of FNPs compared to the positive control (Fb suspension i.n.) across all time points.

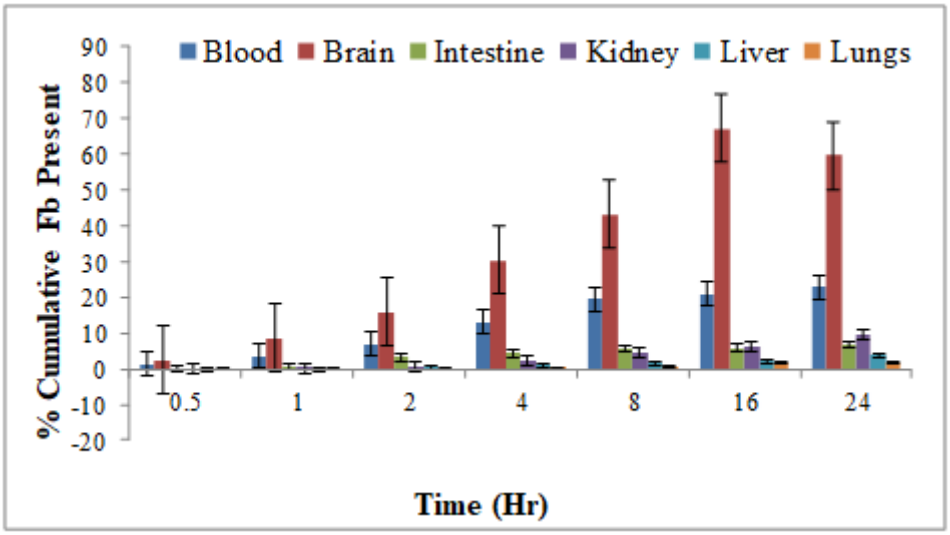

Figure 9. Biodistribution Studies Fb after i.n. administration of FNP.

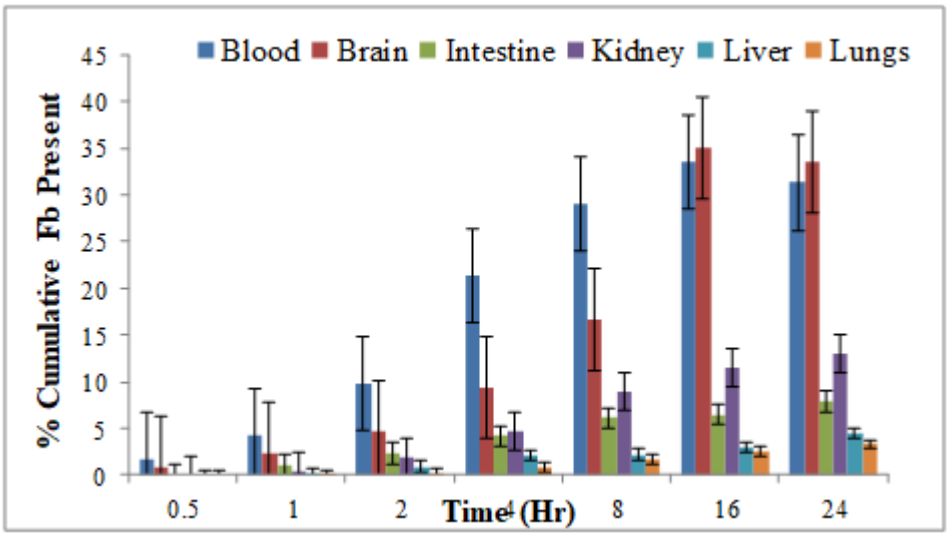

Figure 10. Biodistribution Studies of Fb after i.n. administration of Positive Control (Fb suspension)

Conclusion and Future prospects

In this work, we discussed the ionic cross-linking technique used to create FNPs advantage of nose-to-brain delivery of nanoparticulate formulation against simple suspension of drug. Animals given varying doses of this formulation showed much higher drug concentrations in the brain and significantly lower concentrations in other organs. It follows that Fb-loaded nanosuspension can enhance brain drug concentration by offering direct nose-to-brain transport. It is expected that intranasal administration of a large dose of nanoparticulate formulation rapidly and effectively transported the drug to the brain with little systemic and other side effects, such as first-pass metabolism. The results of this study can be applied to the assessment of felbamate's potential dangers.

References:

1. Agrawal, Mukta et al. 2018. "Nose-to-Brain Drug Delivery: An Update on Clinical Challenges and Progress towards Approval of Anti-Alzheimer Drugs." *Journal of*

controlled release : official journal of the Controlled Release Society 281(April): 139–77. https://doi.org/10.1016/j.jconrel.2018.05.011.

2. Alam, Sanjar et al. 2012. "Development and Evaluation of Thymoquinone-Encapsulated Chitosan Nanoparticles for Nose-to-Brain Targeting: A Pharmacoscintigraphic Study." *International Journal of Nanomedicine* 7: 5705. /pmc/articles/PMC3497894/ (November 8, 2022).
3. Bhattamisra, Subrat K. et al. 2020. "Nose to Brain Delivery of Rotigotine Loaded Chitosan Nanoparticles in Human SH-SY5Y Neuroblastoma Cells and Animal Model of Parkinson's Disease." *International Journal of Pharmaceutics* 579: 119148. https://linkinghub.elsevier.com/retrieve/pii/S0378517320301320 (April 15, 2023).
4. Bhavna et al. 2014. "Donepezil Nanosuspension Intended for Nose to Brain Targeting: In Vitro and in Vivo Safety Evaluation." *International Journal of Biological Macromolecules* 67(June): 418–25. http://dx.doi.org/10.1016/j.ijbiomac.2014.03.022.
5. Borowicz, Kinga K. et al. 2004. "Is There Any Future for Felbamate Treatment?" *Polish journal of pharmacology* 56(3): 289–94. http://www.ncbi.nlm.nih.gov/pubmed/15215558.
6. Cilio, Maria Roberta, Alex I. Kartashov, and Federico Vigevano. 2001. "The Long-Term Use of Felbamate in Children with Severe Refractory Epilepsy." *Epilepsy Research* 47(1–2): 1–7. https://linkinghub.elsevier.com/retrieve/pii/S092012110100290X (April 15, 2023).
7. Fazil, Mohammad et al. 2012. "Development and Evaluation of Rivastigmine Loaded Chitosan Nanoparticles for Brain Targeting." *European Journal of Pharmaceutical Sciences* 47(1): 6–15. https://linkinghub.elsevier.com/retrieve/pii/S0928098712001820 (January 21, 2021).
8. French, J., M. Smith, E. Faught, and L. Brown. 1999. "Practice Advisory: The Use of Felbamate in the Treatment of Patients with Intractable Epilepsy. Report of the Quality Standards Subcommittee of the American Academy of Neurology and the American Epilepsy Society." *Epilepsia* 40(6): 803–8. https://onlinelibrary.wiley.com/doi/10.1111/j.1528-1157.1999.tb00784.x.
9. Haque, Shadabul et al. 2012. "Venlafaxine Loaded Chitosan NPs for Brain Targeting: Pharmacokinetic and Pharmacodynamic Evaluation." *Carbohydrate Polymers* 89(1): 72–79. https://pubmed.ncbi.nlm.nih.gov/24750606/ (January 21, 2021).
10. Kaur, Sarabjit et al. 2018. "Bioengineered PLGA-Chitosan Nanoparticles for Brain Targeted Intranasal Delivery of Antiepileptic TRH Analogues." *Chemical Engineering Journal* 346(November 2017): 630–39. https://doi.org/10.1016/j.cej.2018.03.176.
11. Liu, Shanshan, Shili Yang, and Paul C. Ho. 2018. "Intranasal Administration of Carbamazepine-Loaded Carboxymethyl Chitosan Nanoparticles for Drug Delivery to the Brain." *Asian Journal of Pharmaceutical Sciences* 13(1): 72–81. https://doi.org/10.1016/j.ajps.2017.09.001.
12. Schmidt, Dieter. 1993. "Felbamate: Successful Development of a New Compound for the Treatment of Epilepsy." *Epilepsia* 34 Suppl 7(s7): S30-3. https://onlinelibrary.wiley.com/doi/10.1111/j.1528-1157.1993.tb04592.x.
13. Seju, U., A. Kumar, and K.K. Sawant. 2011. "Development and Evaluation of Olanzapine-Loaded PLGA Nanoparticles for Nose-to-Brain Delivery: In Vitro and in

Vivo Studies." *Acta Biomaterialia* 7(12): 4169–76. http://dx.doi.org/10.1016/j.actbio.2011.07.025.

14. Siegel, Heidi et al. 1999. "The Efficacy of Felbamate as Add-on Therapy to Valproic Acid in the Lennox–Gastaut Syndrome." *Epilepsy Research* 34(2–3): 91–97. https://linkinghub.elsevier.com/retrieve/pii/S0920121198001193 (April 15, 2023).
15. Mandal S, Vishvakarma P. Nanoemulgel: A Smarter Topical Lipidic Emulsion-based Nanocarrier. Indian J of Pharmaceutical Education and Research. 2023;57(3s):s481-s498.
16. Mandal S, Jaiswal DV, Shiva K. A review on marketed Carica papaya leaf extract (CPLE) supplements for the treatment of dengue fever with thrombocytopenia and its drawback. International Journal of Pharmaceutical Research. 2020 Jul;12(3).
17. Bhandari S, Chauhan B, Gupta N, et al. Translational Implications of Neuronal Dopamine D3 Receptors for Preclinical Research and Cns Disorders. *African J Biol Sci (South Africa)*. 2024;6(8):128-140. doi:10.33472/AFJBS.6.8.2024.128-140
18. Tripathi A, Gupta N, Chauhan B, et al. Investigation of the structural and functional properties of starch-g-poly (acrylic acid) hydrogels reinforced with cellulose nanofibers for cu2+ ion adsorption. *African J Biol Sci (South Africa)*. 2024;6(8): 144-153, doi:10.33472/AFJBS.6.8.2024.141-153
19. Mandal S, Bhumika K, Kumar M, Hak J, Vishvakarma P, Sharma UK. A Novel Approach on Micro Sponges Drug Delivery System: Method of Preparations, Application, and its Future Prospective. Indian J of Pharmaceutical Education and Research. 2024;58(1):45-63.
20. Mishra, N., Alagusundaram, M., Sinha, A., Jain, A. V., Kenia, H., Mandal, S., & Sharma, M. (2024). Analytical Method, Development and Validation for Evaluating Repaglinide Efficacy in Type Ii Diabetes Mellitus Management: a Pharmaceutical Perspective. Community Practitioner, 21(2), 29–37. https://doi.org/10.5281/zenodo.10642768
21. Singh, M., Aparna, T. N., Vasanthi, S., Mandal, S., Nemade, L. S., Bali, S., & Kar, N. R. (2024). Enhancement and Evaluation of Soursop (Annona Muricata L.) Leaf Extract in Nanoemulgel: a Comprehensive Study Investigating Its Optimized Formulation and Anti-Acne Potential Against Propionibacterium Acnes, Staphylococcus Aureus, and Staphylococcus Epidermidis Bacteria. Community Practitioner, 21(1), 102–115. https://doi.org/10.5281/zenodo.10570746
22. Khalilullah, H., Balan, P., Jain, A. V., & Mandal, S. (n.d.). Eupatorium Rebaudianum Bertoni (Stevia): Investigating Its Anti-Inflammatory Potential Via Cyclooxygenase and Lipooxygenase Enzyme Inhibition - A Comprehensive Molecular Docking And ADMET. Community Practitioner, 21(03), 118–128. https://doi.org/10.5281/zenodo.10811642
23. Mandal, S. Vishvakarma, P. Pande M.S., Gentamicin Sulphate Based Ophthalmic Nanoemulgel: Formulation and Evaluation, Unravelling A Paradigm Shift in Novel Pharmaceutical Delivery Systems. Community Practitioner, 21(03), 173-211. https://doi.org/10.5281/zenodo.10811540
24. Mandal, S., Tyagi, P., Jain, A. V., & Yadav, P. (n.d.). Advanced Formulation and Comprehensive Pharmacological Evaluation of a Novel Topical Drug Delivery System for the Management and Therapeutic Intervention of Tinea Cruris (Jock Itch). Journal of Nursing, 71(03). https://doi.org/10.5281/zenodo.10811676

25. Mishra, N., Alagusundaram, M., Sinha, A., Jain, A. V., Kenia, H., Mandal, S., & Sharma, M. (2024). Analytical Method, Development and Validation for Evaluating Repaglinide Efficacy in Type Ii Diabetes Mellitus Management: a Pharmaceutical Perspective. Community Practitioner, 21(2), 29–37. https://doi.org/10.5281/zenodo.10642768
26. Singh, M., Aparna, T. N., Vasanthi, S., Mandal, S., Nemade, L. S., Bali, S., & Kar, N. R. (2024). Enhancement and Evaluation of Soursop (Annona Muricata L.) Leaf Extract in Nanoemulgel: a Comprehensive Study Investigating Its Optimized Formulation and Anti-Acne Potential Against Propionibacterium Acnes, Staphylococcus Aureus, and Staphylococcus Epidermidis Bacteria. Community Practitioner, 21(1), 102–115. https://doi.org/10.5281/zenodo.10570746
27. Gupta, N., Negi, P., Joshi, N., Gadipelli, P., Bhumika, K., Aijaz, M., Singhal, P. K., Shami, M., Gupta, A., & Mandal, S. (2024). Assessment of Immunomodulatory Activity in Swiss Albino Rats Utilizing a Poly-Herbal Formulation: A Comprehensive Study on Immunological Response Modulation. Community Practitioner, 21(3), 553–571. https://doi.org/10.5281/zenodo.10963801
28. Mandal S, Vishvakarma P, Bhumika K. Developments in Emerging Topical Drug Delivery Systems for Ocular Disorders. Curr Drug Res Rev. 2023 Dec 29. doi: 10.2174/0125899775266634231213044704. Epub ahead of print. PMID: 38158868.
29. Abdul Rasheed. A. R, K. Sowmiya, S. N., & Suraj Mandal, Surya Pratap Singh, Habibullah Khallullah, N. P. and D. K. E. (2024). In Silico Docking Analysis of Phytochemical Constituents from Traditional Medicinal Plants: Unveiling Potential Anxiolytic Activity Against Gaba, Community Practitioner, 21(04), 1322–1337. https://doi.org/10.5281/zenodo.11076471
30. Thakkar, Karan et al. 2015. "The Rise and Fall of Felbamate as a Treatment for Partial Epilepsy – Aplastic Anemia and Hepatic Failure to Blame?" *Expert Review of Neurotherapeutics* 15(12): 1373–75. http://dx.doi.org/10.1586/14737175.2015.1113874.
31. Tong, Gui-Feng, Nan Qin, and Li-Wei Sun. 2017. "Development and Evaluation of Desvenlafaxine Loaded PLGA-Chitosan Nanoparticles for Brain Delivery." *Saudi Pharmaceutical Journal* 25(6): 844–51. http://dx.doi.org/10.1016/j.jsps.2016.12.003.
32. Tzeyung, Angeline et al. 2019. "Fabrication, Optimization, and Evaluation of Rotigotine-Loaded Chitosan Nanoparticles for Nose-To-Brain Delivery." *Pharmaceutics* 11(1): 26. http://www.mdpi.com/1999-4923/11/1/26.
33. Wen, Ziyi et al. 2011. "Brain Targeting and Toxicity Study of Odorranalectin-Conjugated Nanoparticles Following Intranasal Administration." *Drug Delivery* 18(8): 555–61. https://pubmed.ncbi.nlm.nih.gov/21812752/ (January 21, 2021).
34. Xiao, Xiao-Yu et al. 2016. "Evaluation of Neuroprotective Effect of Thymoquinone Nanoformulation in the Rodent Cerebral Ischemia-Reperfusion Model." *BioMed research international* 2016: 2571060. https://www.hindawi.com/journals/bmri/2016/2571060/.